SCATTERED-LIGHT PHOTOELASTICITY IN THE STUDY OF INTERNAL CRACKS IN THREE-DIMENSIONAL BODIES

L. S. Srinath, K. S. S. Aradhya and K. Chandru

Department of Mechanical Engineering, Indian Institute of Science, Bangalore 560012, India

ABSTRACT

The newly developed techniques of scattered-light photoelasticity have been used to analyse crack problems in three-dimensional bodies in a completely non-destructive manner. The stress-distributions around a penny-shaped crack in a thick beam under pure bending and the corresponding stress intensity factors are reported in this paper. The experimental results are compared with the available theoretical solutions.

KEYWORDS

Fracture mechanics, Internal cracks, Stress intensity factor, Scattered-light photoelasticity, Non-destructive analysis.

INTRODUCTION

In fracture mechanics, the analysis of problems involving embedded flaws in three-dimensional bodies pose great difficulties. A limited number of analytical work that has been done on flaws of elliptical and penny shapes are reported (Sneddon, 1946; Kassir and Sih, 1966; Smith and Alavi, 1971; Shah and Kobayashi, 1972). However, there are no experimental investigations so far in support of these analytical works. The present paper discusses the results of an experimental investigation of stresses near a penny-shaped crack in a beam under pure bending. Values of Stress Intensity Factors (SIF's) have been obtained from these stress distributions.

THE MODEL

Figure 1 shows the details of making a beam with an embedded crack. A penny-shaped crack was created by cementing two araldite blocks as shown in Figs. 1(a) and (b). Hot set material composed of CY-230 resin and HT-901 hardner taken in proportions of 100:45 by weight was used in making the specimen. The values of Young's Modulus and Poisson's ratio for the material at room temperature were 28,800 kgf/cm^2 and 0.31 respectively. The material fringe value at room temperature was 13.0 kgf/fringe/cm. The beam was subjected to pure bending

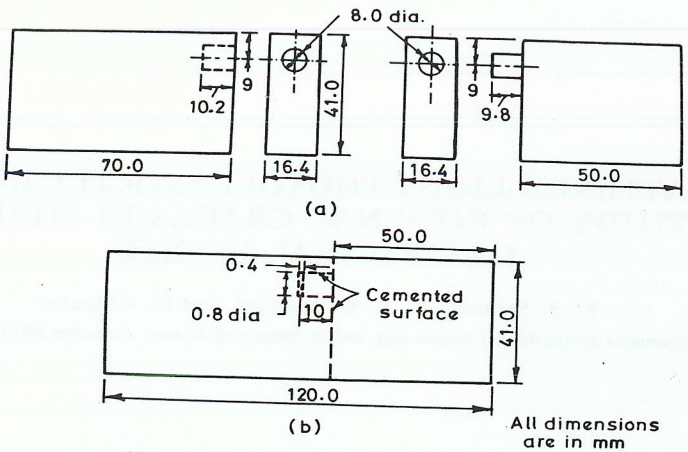

Fig. 1. Details of beam making.

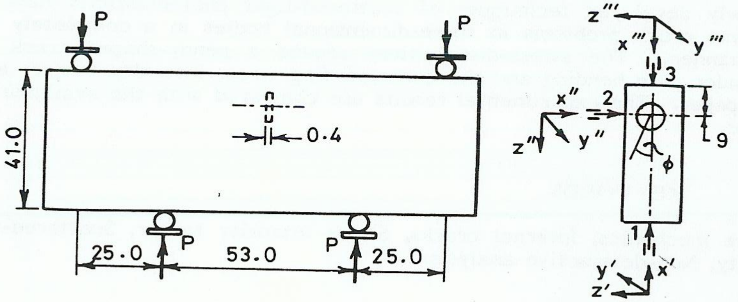

Fig. 2. Beam with penny-shaped crack under pure bending.

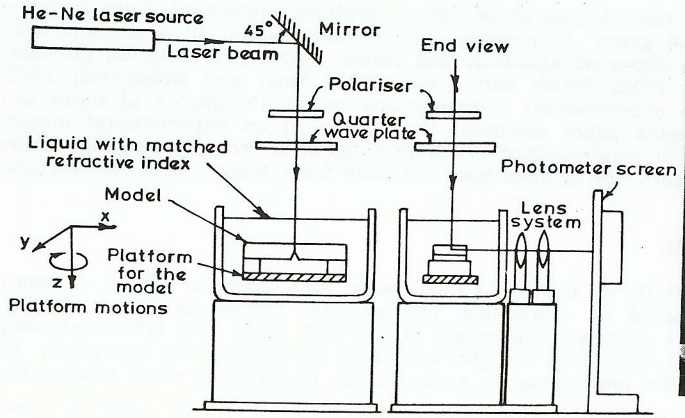

Fig. 3.

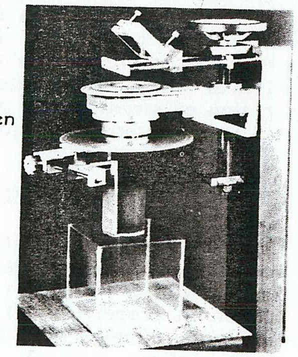

Fig. 4.

so that the crack was under Mode I loading (Fig. 2). The impressed B.M. was 440 kgfcm.

SCATTERED-LIGHT PHOTOELASTICITY

The techniques of scattered-light photoelasticity were used advantageously to explore the stresses since investigations can be conducted on the models under live loads at room temperature conditions in a completely non-destructive manner. The currently available scattered-light techniques completely take care of the problem of rotation of secondary principal stress axes along the light path using the concept of optically equivalent model and enable one to determine the associated photoelastic parameters along the light path using which one can calculate the corresponding secondary principal stress differences and their axes (Srinath, Godbole and Keshavan, 1979). Figures 3 and 4 show the schematic diagram and the photograph of the scattered-light polariscope respectively. The source of light was a 8 mW He-Ne laser. The light intensities were monitored by a photometric unit. Determination of fractional fringe orders was done using reversed Friedel's method.

STRESS DISTRIBUTIONS

Stresses were explored along directions 1, 2 and 3 as indicated in Fig. 2, from the fringe order distributions observed along these directions. Figures 5, 6 and 7 show the fringe patterns observed along the direction 1. Figure 5 corresponds to full order fringes, Fig. 6 to half order fringes and Fig. 7 to a sheet of circularly polarized light. Similarly, Figs. 8, 9 and 10 are the corresponding frige patterns for incident light along direction 3 (Fig. 2). Figure 11 shows the plot of fringe order distributions along directions 1 and 3. The slope of these curves at any point is proportional to the stress $(\sigma_y - \sigma_z)$ at that point. Figure 12 shows the distribution of $(\sigma_y - \sigma_z)$ stress along directions 1 and 3. Figures 13 to 16 give similar informations along direction 2. From the stress distributions obtained, one can calculate the Stress Intensity Factors as discussed below.

CALCULATION OF STRESS INTENSITY FACTORS

Among the various methods suggested to determine SIF, the following were used in the present investigation.

1. Average stress method (Marloff and others, 1971)

From Westergaard's equations (Paris and Sih, 1965) for the elastic stress field in the near vicinity of a sharp crack-tip under Mode I loading one obtains for $\theta = 0$ the expression,

$$\sigma_y = [K_I/(2\pi)^{1/2}]\, r^{-1/2} \qquad (1)$$

From the straight line part of the plot of σ_y as a function of $1/\sqrt{r}$ one gets the value of K_I.

2. Differencing technique (Aradhya and others, 1981)

Fig. 5.

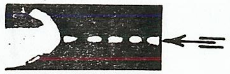

Fig. 8.

Fig. 6.

Fig. 9

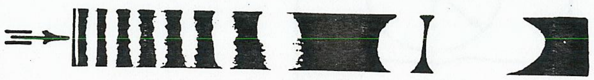

Fig. 7

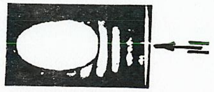

Fig. 10

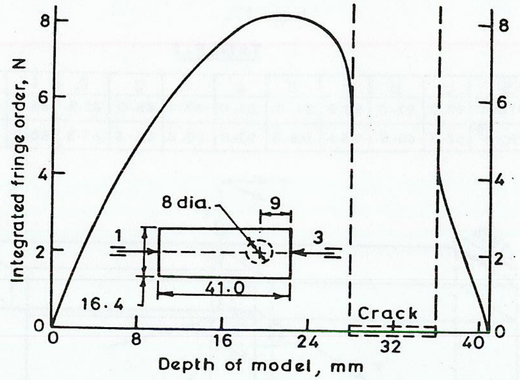

Fig. 11. Integrated fringe order (N) variation along the light path (x) for the directions 1 and 3 (Fig. 2.).

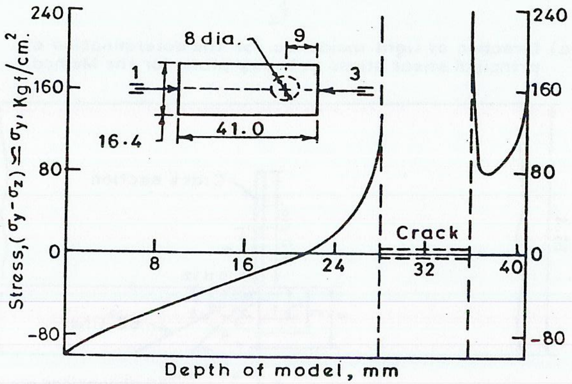

Fig. 12. Variation of Stress (σ_y - σ_z) ≃ σ_y along the directions 1 and 3. (Fig. 2)

Fig. 13.

Fig. 14.

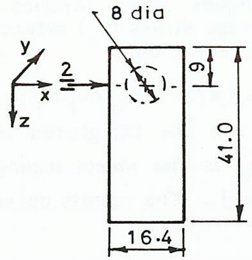

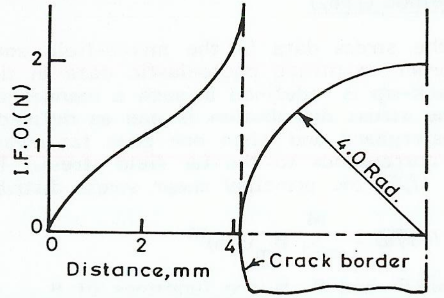

Fig. 15. Integrated fringe order (N) variation along the light path (x) for the direction 2 (Fig. 2).

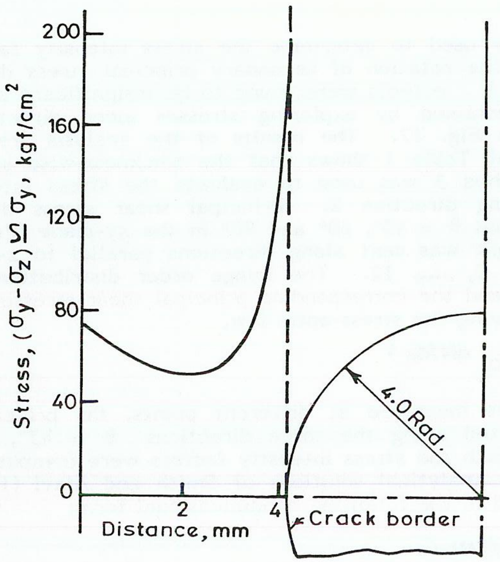

Fig. 16. Variation of stress (σ_y - σ_z) ≃ σ_y along direction 2 (Fig. 2).

This method developed to determine the stress intensity factor using scattered-light photoelastic techniques when rotation of secondary principal stress directions and the thickness-wise stress (σ_z) effects along the light path are negligible, makes use of the following equation,

$$(K_I)_{ij} = (\pi/2)^{1/2} F_\sigma (N_i - N_j)/(r_i^{1/2} - r_j^{1/2}) \qquad (2)$$

where N_i and N_j are the integrated fringe orders at distances r_i and r_j in the singular zone, $(K_I)_{ij}$ is the stress intensity factor obtained by combining informations at points i and j . The results obtained are statistically conditioned.

3. Prabhu and others method (1982)

This method utilizes the stress data in the mixed-field zone which is 'not-too-near' the crack. In order to utilize photoelastic data in this zone the state of stress ahead of the crack-tip is redefined in such a manner that when one approaches the ctrack-tip, the stress distribution is one as defined by the stress singularity equations of Westergaard and when one goes far away from the crack-tip, the stress distribution corresponds to the far field stress. Noting that the order of stress singularity is $1/\sqrt{r}$, the principal shear stress distribution can be written as,

$$\sigma_1 - \sigma_2 = (K/\sqrt{r/a}) + \sum_{m=1}^{M} B_m (r/a)^m \qquad (3)$$

where $K = (K_I/\sqrt{2\pi a}) \sin\theta$ and B_m's are functions of θ . One can now obtain photelastic data at (M+1) points along any fixed θ ($\theta \neq 0$) and form (M+1) simultanesous equations in K, B_1, B_2, ..., etc. The solution of these equations gives information regarding K and B_m's from which K_I can be obtained.

Methods 1 and 2 were used to determine the stress intensity factors along directions 1 and 3 since the rotation of secondary principal stress directions and the thicknesswise stress (σ_z) effects were found to be insignificant along these directions. (This was ascertained by exploring stresses along directions 1,2,3,4 and 1',2',3' as depicted in Fig. 17. The results of the analysis are shown in Table 1. An examination of Table 1 shows that the thickness-wise stress effects are inconsequential). Method 3 was used to evaluate the stress intensity factor for stress distribution along direction 2. Principal shear stress distributions were obtained along directions θ = 45°, 60° and 90° in the xy-plane (Fig. 18). For this purpose the ray of light was sent along directions parallel to z-axis and passing through the points 1, 2, ..., 12. The fringe order distributions were obtained along these directions and the corresponding principal shear stresses in the xy-plane were computed by applying the stress-optic law,

$$\sigma_1 - \sigma_2 = F_\sigma (dN/dz) \qquad (4)$$

From the stress values measured at different points, the principal shear stress distributions were plotted along the three directions θ = 45°, 60° and 90° (as functions of r) from which the stress intensity factors were computed. For purposes of comparing with the analytical solutions of Smith and Alavi (1971), the results obtained were expressed in the following nondimensional form:

$$Y = (\sqrt{\pi} I K_I)/2Mb\sqrt{a} \qquad (5)$$

where Y is nondimensional SIF, K_I is experimentally determined SIF (in kgfcm$^{-3/2}$) M is the applied B.M. (in kgfcm), I is the M.I. of the section of the beam (in cm^4)

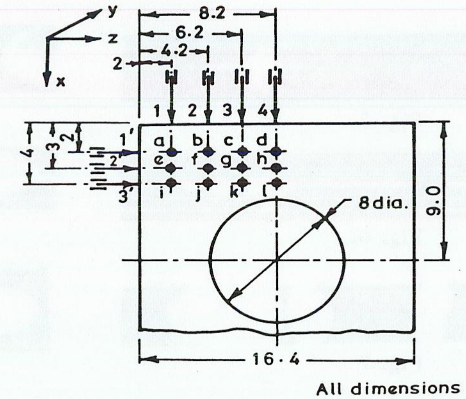

Fig. 17.

TABLE.1

POINTS	a	b	c	d	e	f	g	h	i	j	k	l
$(\sigma_y - \sigma_z)$ kgf/cm^2	97.0	92.0	92.0	92.0	87.0	85.0	85.0	82.5	85.5	81.0	78.5	79.0
$(\sigma_y - \sigma_x)$ kgf/cm^2	97.5	93.6	86.6	88.8	92.0	80.8	86.6	87.5	90.0	81.5	83.5	85.0

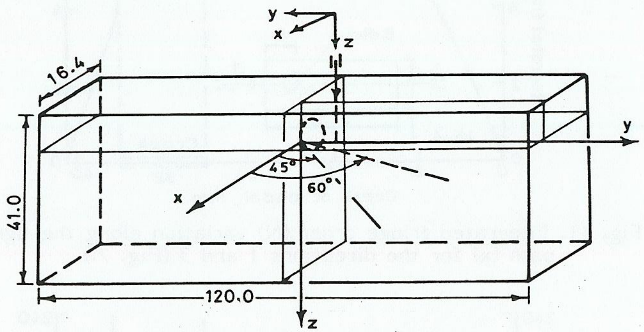

(a). Direction of light incidence for the determination of principal shear stress in the xy plane for the Method.3

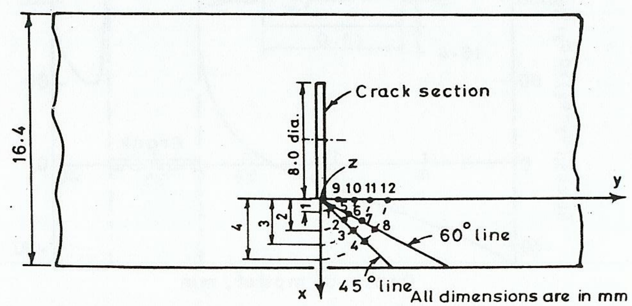

(b). Points at which principal stresses are measured in the xy plane

Fig. 18.

and a and b are the radius of the crack and semi-depth of the beam (in cm) respectively. Table 2 shows the comparison of the results obtained with the analytical solutions of Smith and Alavi (1971).

TABLE 2 Nondimensional SIF's $[Y = (\sqrt{\pi}K_I)2Mb\sqrt{a}]$.

Directions (Fig. 2)	Present Investigation		Prabhu and others method Eq. (3)	Results of Smith and Alavi (1971)
	Avg. stress method Eq. (1)	Differencing Technique Eq. (2)		
$\phi = 0°$	50.0	50.2	-	50.42
$\phi = 90°$	-	-	52.4	52.85
$\phi = 180°$	55.0	55.5	-	55.64

OBSERVATIONS

There is a good agreement between the experimental and analytical results, the maximum deviation being 4% . The accuracy of the results obtained shows that the scattered-light photoelastic method is an effective non-destructive tool in the study of internal crack problems in three-dimensional bodies. The singular stress field has the bounds ($0.075 < r/a < 0.3$) for methods 1 and 2. The mixed field region used in the method 3 has the bounds ($0.25 < r/a < 1$). The thickness-wise stress effects were found to be insignificant along directions 1 and 3 (Fig. 2) and the stresses measured along these directions were predominantly the stretching stresses due to bending.

REFERENCES

Aradhya, K. S. S., Srinivasa Murthy, N. and Srinath, L. S. (1981). Determination of Mode I Stress Intensity Factors for Three-dimensional Photoelastic Notched Specimen under Live-load and Stress-frozen conditions, Proc. 26th Congress of ISTAM, Coimbatore (India).

Kassir, M. K. and Sih, G. C. (1966). Three dimensional crack problems, International Publishing, Leyden.

Marloff, R. H., Leven, M. M., Ringler, T. N. and Johnson, R. L. (1971). Photoelastic determination of stress-intensity factors, Experimental Mechanics, Vol.11,529-539.

Paris, P. C. and Sih, G. C. (1965). Fracture toughness testing and its applications, ASTM STP 381, 30-83.

Prabhu, M. M., Godbole, P. B., Bhave, S. K. and Srinath, L. S. (1982). Modified approach to determine Mode I stress-intensity factor using photoelasticity, Proc. 1982 Joint Conference on Experimental Mechanics (SESA/JSME), Hawaii.

Shah, R. C. and Kobayashi, A. S. (1972). Stress-intensity factor for an elliptical crack approaching the surface of a plate in bending, ASTM STP 513,3-21.Smith, F. W. and Alavi, M. J. (1971). Stress-intensity factors for a penny-shaped crack in a half space. Engineering Fracture Mechanics, Vol.3, 241-254.

Sneddon, I. N. (1946). The distribution of stress in the neighbourhood of a crack in an elastic solid. Proc. Roy. Soc. London, A187, 229-260.

Srinath, L. S., Godbole, P. B. and Keshavan, S. Y. (1979). A new scattered-light method to determine stresses near an interior crack-tip, Proc. IUTAM Symp. on Optical Methods in Mech. of Solids, France, 91-102.